TFE3 Fusions Activate MET Signaling by Transcriptional Up-regulation, Defining Another Class of Tumors as Candidates for Therapeutic MET Inhibition

Masumi Tsuda,[1] Ian J. Davis,[2] Pedram Argani,[3] Neerav Shukla,[1] Gael G. McGill,[2] Makoto Nagai,[1] Tsuyoshi Saito,[1] Marick Laé,[1] David E. Fisher,[2] and Marc Ladanyi[1,4]

[1]Department of Pathology, Memorial Sloan-Kettering Cancer Center, New York, New York; [2]Melanoma Program in Medical Oncology, Dana-Farber Cancer Institute, Boston, Massachusetts; [3]Department of Pathology, The Johns Hopkins Hospital, Baltimore, Maryland; and [4]Human Oncology and Pathogenesis Program, Memorial Sloan-Kettering Cancer Center, New York, NY

Abstract

Specific chromosomal translocations encoding chimeric transcription factors are considered to play crucial oncogenic roles in a variety of human cancers but the fusion proteins themselves seldom represent suitable therapeutic targets. Oncogenic TFE3 fusion proteins define a subset of pediatric renal adenocarcinomas and one fusion (ASPL-TFE3) is also characteristic of alveolar soft part sarcoma (ASPS). By expression profiling, we identified the *MET* receptor tyrosine kinase gene as significantly overexpressed in ASPS relative to four other types of primitive sarcomas. We therefore examined *MET* as a direct transcriptional target of ASPL-TFE3. ASPL-TFE3 binds to the *MET* promoter and strongly activates it. Likewise, PSF-TFE3 and NONO-TFE3 also bind this promoter. Induction of *MET* by ASPL-TFE3 results in strong MET autophosphorylation and activation of downstream signaling in the presence of hepatocyte growth factor (HGF). In cancer cell lines containing endogenous TFE3 fusion proteins, inhibiting MET by RNA interference or by the inhibitor PHA665752 abolishes HGF-dependent MET activation, causing decreased cell growth and loss of HGF-dependent phenotypes. MET is thus a potential therapeutic target in these cancers. Aberrant transcriptional up-regulation of *MET* by oncogenic TFE3 fusion proteins represents another mechanism by which certain cancers become dependent on MET signaling. The identification of kinase signaling pathways transcriptionally up-regulated by oncogenic fusion proteins may reveal more accessible therapeutic targets in this class of human cancers. [Cancer Res 2007;67(3):919–29]

Introduction

The *ASPL-TFE3* fusion arising from a t(X;17)(p11.2;q25.3) characterizes two distinct human cancers, alveolar soft part sarcoma (ASPS), where it is present in all cases, as well as a newly defined subset of pediatric renal adenocarcinomas (1, 2). ASPS is an uncommon chemoresistant sarcoma typically presenting as an extremity tumor in an adolescent or young adult; it is associated with a high risk of metastases that may only become clinically apparent many years after initial diagnosis (1). *ASPL-TFE3*–positive renal carcinomas form a small proportion of adult renal carcinomas but are overrepresented in children and young adults; given their very recent description, their long-term clinical course remains unclear at this time but metastases have been reported (2). *ASPL-TFE3* renal carcinomas represent just one of several subtypes of renal carcinoma characterized by translocations involving *TFE3*. These include *PRCC-TFE3* (3–5), *PSF-TFE3*, and *NONO-TFE3* (6), among others, and together they make up a distinctive type of renal carcinoma recently designated translocation carcinomas of the kidney (7). These renal cancers are now being increasingly recognized in adults as well (8).

TFE3 is a member of the microphthalmia-TFE basic helix-loop-helix leucine zipper transcription factor subfamily. The normal cellular role of ASPL (ASPSCR1) remains to be fully elucidated but it may function at least in part as a regulator of intracellular trafficking of the GLUT4 glucose transporter (9). The ASPL-TFE3 fusion replaces the NH_2-terminal portion of TFE3 by ASPL sequences while retaining the TFE3 DNA-binding region, activation domain, and nuclear localization signal (1). The ASPL-TFE3 fusion protein functions as a stronger transactivator compared with native TFE3 at several promoters (10). These findings suggest that inappropriate target gene transactivation by ASPL-TFE3 may contribute to its oncogenic properties in ASPL-TFE3–associated tumors. Other TFE3 fusion proteins have also been shown to function as aberrant transcription factors (11, 12).

Here, we provide evidence that ASPL-TFE3–mediated direct transcriptional up-regulation of the MET receptor tyrosine kinase triggers dramatic activation of downstream signaling pathways. The depletion of MET by RNA interference or its functional inhibition by the selective inhibitor PHA665752 abolishes HGF-stimulated signaling pathways, leading to loss of various tumorigenic phenotypes in ASPL-TFE3–associated renal carcinoma cells, including cell proliferation, adhesion, cell motility, and Matrigel invasion. We also provide evidence supporting a similar role for other TFE3 fusion proteins. These findings point to an important role for MET in the pathobiology of human cancers with *TFE3* fusions and highlight MET as a more tractable therapeutic target in these cancers than the fusion proteins themselves.

Materials and Methods

Cells

The following cell lines were used: 293T human embryonic kidney, Cos-7 African Green Monkey kidney, HeLa human cervix adenocarcinoma, A673 Ewing sarcoma (13), HS-SY-II synovial sarcoma (14), Fuji synovial sarcoma (15), RH30 alveolar rhabdomyosarcoma, MCF-7 breast adenocarcinoma,

Note: Supplementary data for this article are available at Cancer Research Online (http://cancerres.aacrjournals.org/).

D.E. Fisher is a recipient of a Doris Duke Distinguished Clinical Investigator Award.

Requests for reprints: Marc Ladanyi, Department of Pathology, Memorial Sloan-Kettering Cancer Center, Room S-801, 1275 York Avenue, New York, NY 10021. Phone: 212-639-6369; Fax: 212-717-3515; E-mail: ladanyim@mskcc.org.

©2007 American Association for Cancer Research.

doi:10.1158/0008-5472.CAN-06-2855

FU-UR-1 renal carcinoma (gift of Dr. M. Ishiguro, Fukuoka University School of Medicine, Fukuoka, Japan; ref. 16), and the renal carcinoma lines UOK109 and UOK145 (gift of Dr. M. Linehan, National Cancer Institute, Bethesda, MD; ref. 6). Cell culture conditions are provided in Supplementary Methods. To establish ASPL-TFE3 inducible cell lines, T-Rex 293 cells (Invitrogen, Carlsbad, CA) were transfected with DNA of pcDNA4/TO/myc-His, ASPL-TFE3 type 1/TO, or ASPL-TFE3 type 2/TO. After 48 h, the cells were treated with 0.2 mg/mL zeocin (Invitrogen), and drug-resistant colonies were isolated. The expression of ASPL-TFE3 was induced by 1 μg/mL tetracycline (Invitrogen).

Antibodies

MET (C-12 and C-28) and actin (I-19) antibodies were from Santa Cruz Biotechnology (Santa Cruz, CA); Gab1 antibody was from Upstate (Lake Placid, NY). Antibodies against phosphorylated MET (Y1234/Y1235 and Y1349), phosphorylated Gab1 (Y307), phosphorylated RAF (S338), mitogen-activated protein kinase (MAPK) and phosphorylated MAPK (T202/Y204), Akt and phosphorylated Akt (S473, 587F11), signal transducers and activators of transcription 3 (Stat3) and phosphorylated Stat3 (Y705), epidermal growth factor receptor (EGFR) and phosphorylated EGFR (Y845 and Y1068), and phosphorylated myc (T58/S62) were from Cell Signaling (Beverly, MA). The antibody against Crk was from Transduction Laboratories (Lexington, KY); human HGF antibody was from R&D Systems (Minneapolis, MN); myc antibody was from Invitrogen; Flag-M2 with or without horseradish peroxidase was from Sigma (Saint Louis, MO).

Plasmids

cDNAs of *ASPL-TFE3* type 1 or type 2 (1) and wild-type *TFE3* were amplified by PCR and cloned into pcDNA4-myc-His expression vector (Invitrogen). The promoter region of *MET* was delineated using Gene2 Promoter software (Genomatix Software GmbH, Munich, Germany), and a fragment extending 500 bp upstream from the transcription start site was amplified by PCR and cloned into pGL3basic (Promega, Co., Madison, WI). The expression plasmids for Ras V12 and Ras N19 were generous gifts from Dr. S. Tanaka (Hokkaido University, Sapporo, Japan).

Protein Expression

Immunoprecipitation and immunoblotting. Western blotting and the detection of protein-protein interactions by coimmunoprecipitation were carried out using standard techniques, as described in Supplementary Methods.

Immunohistochemistry. Formalin-fixed, paraffin-embedded whole sections or tissue microarray sections of ASPS and *ASPL-TFE3* renal carcinomas were immunostained with MET polyclonal antibody (C-28; Santa Cruz Biotechnology) at 1:3,000 dilution with EDTA pretreatment or with HGF antibody (R&D Systems). Staining for MET and HGF in these *ASPL-TFE3*–containing tumors was compared with that seen in tissue microarray sections of other translocation-associated sarcomas, including synovial sarcoma, Ewing sarcoma, alveolar rhabdomyosarcoma, and desmoplastic small round cell tumor.

Luciferase Reporter Assay

The activation of the *MET* promoter construct was examined using the Dual Luciferase Promoter Assay System (Promega), using standard techniques, as described in Supplementary Methods.

MET Promoter Chromatin Immunoprecipitation Assay for ASPL-TFE3

This was done using the chromatin immunoprecipitation (ChIP) Assay kit from Upstate Biotechnology (Lake Placid, NY), as described in detail in Supplementary Methods. ChIP-purified DNA was analyzed by PCR for the presence of *MET* promoter sequences, by using the following primers: forward, 5′-CGCTTTGTGAGCAGATGCGG; reverse, 5′-AGCGGCGCAAGGACCACACG.

MET Promoter ChIP Assays in UOK109 and UOK145 Cells

UOK109 and UOK145 chromatin were prepared as described (17): immunoprecipitated with rabbit polyclonal anti-TFE3 (P-16, Santa Cruz), anti-TFEB (V-17, Santa Cruz), anti–microphthalmia transcription factor (MITF; rabbit polyclonal), or anti–glutathione *S*-transferase (GST); and amplified with *MET* promoter primers (5′-TTCTGCGGTGCCCAAATCTCT-3′ and 5′-TGTCTGTCTGCCTCGCGTGCTGTC-3′) or control downstream primers (5′-GAACGTAAAATGTGTCGCTC-3′ and 5′-CTCTGTCAGATAAGA AATTCCTTAG-3′) with Advantage GC (Clontech, Mountain View, CA).

Quantitative Real-time Reverse Transcription-PCR

Total RNA was isolated from the cells using RNeasy kit (Qiagen, Valencia, CA). First strand cDNA was synthesized from 5 μg total RNA by SuperScript II reverse transcriptase (Invitrogen). Real-time reverse transcription-PCR (RT-PCR) for *MET* was done using iCycler (Bio-Rad, CA). The amounts of the various target genes and *TATA-box binding protein* (*TBP*) gene as an endogenous control were quantified by standard curves obtained from serial dilutions of standard plasmids. The sequences for primers and probes were as follows: *c-MET* forward primer, 5′-CATGCCGACAAGTGCAGTA; *c-MET* reverse primer, 5′-TCTTGCCATCATTGTCCAAC; *c-MET* probe, CCAGGCAGTGCAGCATGTAGTGAT; *TBP* forward primer, 5′-GCATATTTTCTTGCTGCCAGTCT; *TBP* reverse primer, 5′-ACCACGGCACTGATTTTCAGTT; *TBP* probe, 5′-ACTGTTCTTCACTCTCTTGGCTCCTGTGCA. Standard plasmids were generated by cloning cDNA fragments of *MET* and *TBP* into the pCRII TOPO plasmid (Invitrogen).

MET Inhibition

Selective MET inhibitor. PHA665752 (kindly provided by J. Christensen, Pfizer, Inc., La Jolla, CA; ref. 18) was dissolved in DMSO and used at the concentrations described below.

RNA interference. For experiments with FU-UR-1 cells, small interfering RNAs (siRNA) targeting *MET* mRNA were obtained from Dharmacon, Inc. (Lafayette, CO) and used according to the manufacturer's instructions. We used a pool of four *MET*-specific 21-nucleotide double-stranded RNA oligonucleotides each forming a 19-bp duplex core with 2-nucleotide 3′ overhangs. *MET* siRNA duplexes were transiently transfected into FU-UR1 cells using HiPerFect transfection reagent (Qiagen). The reagent used for transfection was added in MOCK cells, and negative control cells were transfected by nonspecific control pool siRNA (Dharmacon). For experiments with UOK109 and UOK145 cells, *MET* short hairpin RNA (shRNA) sequences (19) were isolated from the parental pSuper vector by *Eco*RI and *Xho*I digestion and cloned into p(si)^2-puro (20). Cells were infected with retrovirus produced as described (20) and selected with puromycin (2 μg/mL).

Measurement of Growth Rates

For FU-UR1 cells, 1×10^5 cells were seeded onto 60-mm-diameter plates and were treated the following day with or without PHA665752, PD98059, LY294002, and rapamycin at the doses indicated below. To assess cell viability, the numbers of cells were counted at 4 days using a hemocytometer. The effects of PHA665752 and/or rapamycin on cell proliferation were examined every other day for 10 days. For UOK109, colony counts were done as described (20). For UOK145 cells, cells were fixed and stained with crystal violet and then destained with 10% methanol/10% acetic acid and the absorbance at 595 to 750 nm was measured to quantitate cell survival, as described (20).

Results

***MET* is highly differentially overexpressed in ASPS.** We performed expression profiling using the Affymetrix U133A chips on 16 cases of surgically resected ASPS, all previously confirmed to contain either the *ASPL-TFE3* type 1 or type 2 chimeric transcript (Fig. 1*A*). The global expression profile of the ASPS tumors was compared with that of four other translocation-associated sarcomas, including synovial sarcoma, Ewing sarcoma, alveolar rhabdomyosarcoma, and desmoplastic small round cell tumor. We have observed that differentially expressed genes defined by expression profiling of human cancers with chimeric transcription factors provide an enriched source of candidate transcriptional targets of these specific fusion oncoproteins (21). A similar

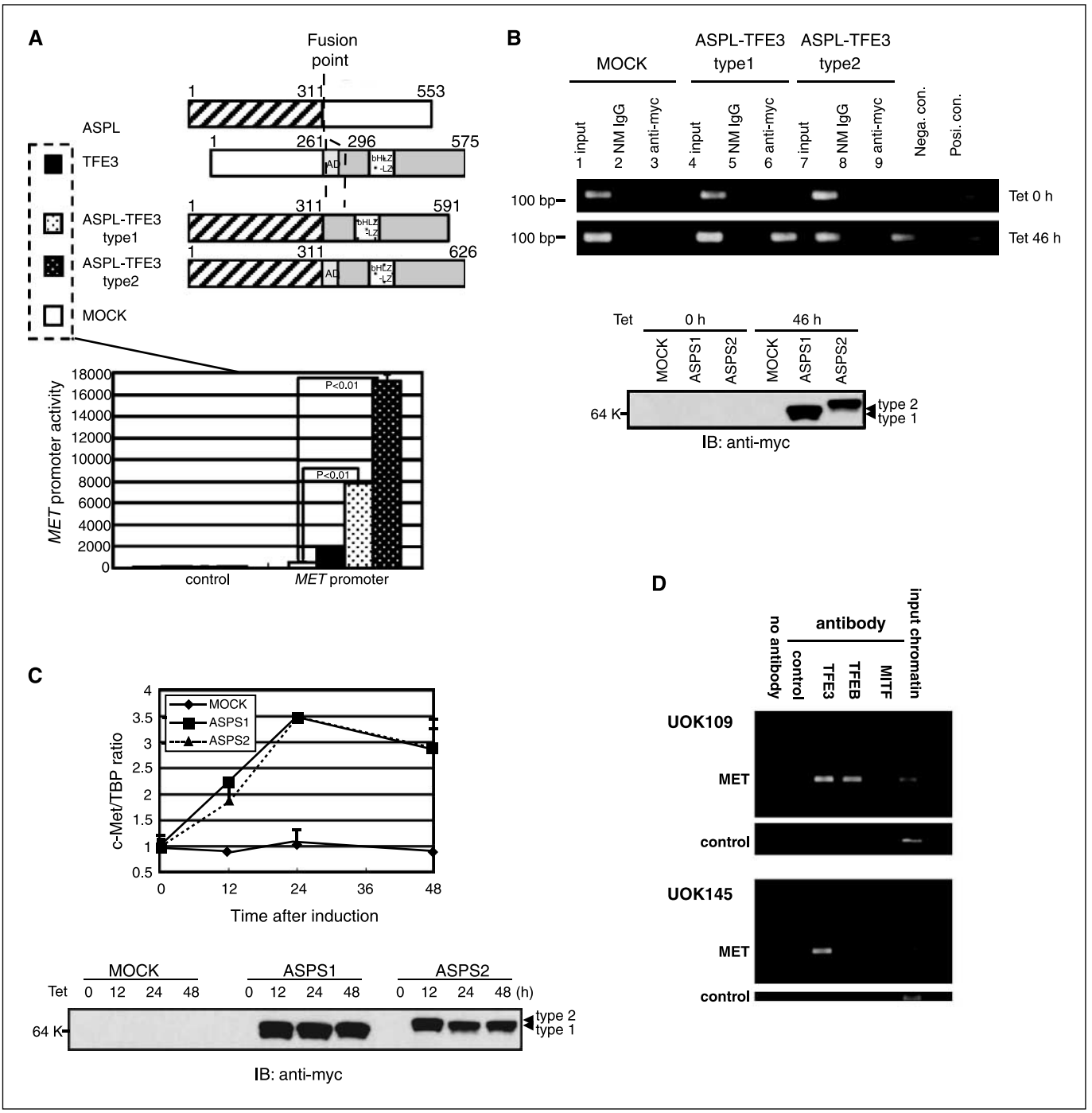

Figure 1. The *MET* promoter is a direct target of ASPL-TFE3. *A,* ASPL-TFE3–mediated transactivation of *MET* promoter. 293T cells were transiently cotransfected with the *MET* promoter reporter plasmid and the expression plasmid for native TFE3, or ASPL-TFE3 type 1 or type 2. MOCK cells were transfected with the empty plasmid. The luciferase activities were normalized to that of cotransfected pRL-TK plasmid. *Columns,* mean from three independent experiments; *bars,* SD. Statistical analyses were done by Student's *t* test, and the luciferase results for ASPL-TFE3 type 1 or type 2 were significantly different from that of MOCK-transfected cells at $P < 0.01$. The pGL3-basic reporter plasmid without *MET* promoter was used as negative control (*left side*). The schematic structures of ASPL, TFE3, and ASPL-TFE3 chimeric proteins (type 1 and type 2) are shown. *Dotted line,* the fusion points in the chimeric gene products. *Numbers,* amino acid residues. *AD,* transcription activation domain. *B,* chromatin immunoprecipitation assays were done to confirm the binding of ASPL-TFE3 to the *MET* promoter. MOCK, ASPL-TFE3 type 1– or type 2–inducible 293 cell lines were treated with 1 μg/mL tetracycline for 46 h, and the cell lysates were treated as described in Materials and Methods. PCR was done to detect the endogenous *MET* promoter sequences in chromatin-DNA complexes containing ASPL-TFE3. *Lanes 1, 4,* and *7,* the amplification in total input DNA before immunoprecipitation. *Lanes 2, 5,* and *8,* PCR amplification in samples precipitated with normal mouse IgG as negative control. *Lanes 3, 6,* and *9,* the presence of *MET* promoter sequences in ASPL-TFE3–containing chromatin-DNA complexes immunoprecipitated with anti-myc antibody. The expression levels of ASPL-TFE3 after tetracycline treatment were examined by immunoblotting using anti-myc antibody. *C,* the relative expression of *MET* mRNA was analyzed by quantitative PCR after ASPL-TFE3 induction in 293 cells, and this was normalized to that of the *TBP* control gene. The expression levels of ASPL-TFE3 after tetracycline treatment were examined by immunoblot using anti-myc antibody. *D,* the *MET* promoter is also bound by other TFE3 fusion proteins. Chromatin preparations isolated from UOK109 and UOK145 cells were immunoprecipitated with anti-TFE3, TFEB, or MITF antibodies or a control antibody (anti-GST), subjected to PCR with primers specific for the *MET* promoter or a region downstream of the *MET* promoter (*control*) and separated by agarose gel electrophoresis. *Input chromatin,* amplified unfractionated chromatin.

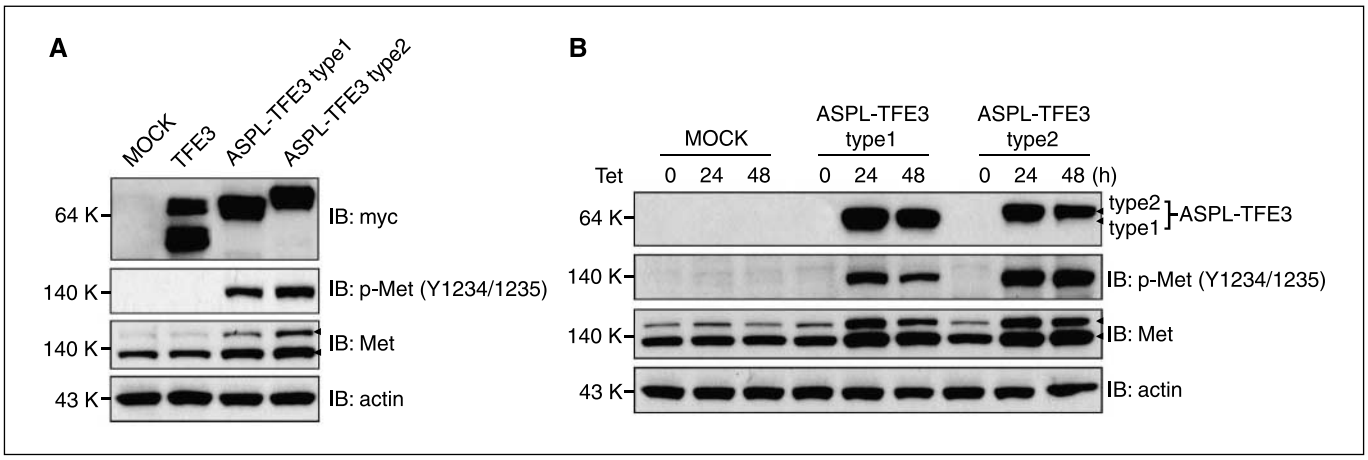

Figure 2. ASPL-TFE3–induced MET expression and its phosphorylation. *A,* 293T cells were transiently transfected with the expression plasmids for MOCK, native TFE3, ASPL-TFE3 type 1, or ASPL-TFE3 type 2, and their expression levels were examined by immunoblotting (*IB*) using anti-myc antibody. The expression of MET and its phosphorylation at Y1234/Y1235 residues were analyzed by immunoblotting with specific antibodies. *Upper arrowhead in the MET immunoblot,* precursor MET; *lower arrowhead,* mature form of MET. *B,* the expression of MET and its phosphorylation at Y1234/1235 residues after ASPL-TFE3 induction were examined by immunoblotting. ASPL-TFE3–inducible 293 cells were treated with 1 μg/mL tetracycline for 24 or 48 h. *Upper arrowhead,* precursor MET; *lower arrowhead,* mature form of MET.

observation has been made in acute leukemias with chimeric transcription factors (22). We have used this approach to identify other direct transcriptional targets of ASPL-TFE3 (10).

Here, to identify ASPL-TFE3 transcriptional targets of potential therapeutic interest, we focused on kinase genes specifically up-regulated in ASPS relative to the other sarcomas listed above. We identified 739 probe sets on the Affymetrix U133A chip corresponding to 432 genes with kinase domains by searches of the annotation database provided by Affymetrix and careful curation based on comprehensive reviews (23, 24) and genome database searches. We examined which kinase genes were most differentially expressed in ASPS relative to the four other sarcomas. This revealed that the *MET* receptor tyrosine kinase gene was among the kinase genes most significantly overexpressed in ASPS compared with the other sarcomas (Supplementary Table S1). The relative fold change of *MET* and its *P* value by Student's *t* test were 4.9 and 2.91×10^{-9}, respectively. This was significant at $P < 0.01$ after Bonferroni correction (a method considerably more stringent that the Benjamini-Hochberg false discovery rate). Based on this analysis, we chose to examine *MET* as a potential ASPL-TFE3 target gene.

***MET* is a direct transcriptional target of ASPL-TFE3.** In standard cotransfection assays, exogenous ASPL-TFE3 type 1 or type 2 fusion protein induced prominent transactivation of an exogenous *MET* promoter construct in 293 cells, significantly higher relative to that of native TFE3, especially in the case of ASPL-TFE3 type 2 (Fig. 1*A*). This reporter was driven by a portion of the *MET* promoter extending 500 bp upstream from its transcription start site. CANNTG, the consensus binding sequence for native TFE3, is also bound by ASPL-TFE3 fusion proteins (10). Therefore, we used ChIP to examine whether ASPL-TFE3 localizes to a portion of the *MET* promoter containing a CANNTG site (CACGTG, ~300 bp upstream from the *MET* transcription start site) using 293 cells with inducible ASPL-TFE3 expression (T-Rex system). This revealed that the myc-tagged ASPL-TFE3 type 1 or type 2 fusion proteins were specifically present at the endogenous *MET* promoter in 293 cells (Fig. 1*B*, *lanes 6* and *9*). To further support ASPL-TFE3–mediated transactivation of *MET* promoter, the levels of *MET* mRNA were examined by real-time quantitative RT-PCR. Induction of ASPL-TFE3 type 1 or its type 2 in 293 cells was followed by a 3.5-fold elevation in the expression level of the endogenous *MET* mRNA relative to that in MOCK cells (Fig. 1*C*).

Other TFE3 fusion proteins also bind specifically to the *MET* promoter. Given the activation of *MET* by ASPL-TFE3, we hypothesized that other renal carcinoma–associated TFE3 fusions may similarly act on the *MET* promoter. The renal carcinoma cell lines UOK109 and UOK145 express the NONO-TFE3 and PSF-TFE3 translocation products, respectively (25). ChIP assays showed reactivity with antibodies directed against TFE3 at the *MET* promoter in both cell lines (Fig. 1*D*). Notably, both of these lines fail to express detectable wild-type TFE3 (ref. 25; and data not shown), supporting the interpretation that TFE3 fusion proteins are occupying the endogenous *MET* promoter in these cells. In addition, native TFEB seemed to be bound to the *MET* promoter in UOK109 cells (Fig. 1*D*), a finding that is consistent with the close biochemical similarity of TFEB to TFE3, as well as its role as a translocated oncogene in other cases of childhood renal carcinoma (26).

ASPL-TFE3 increases MET protein expression and phosphorylation. Next, we used multiple approaches to examine the link between ASPL-TFE3 and the expression level and activation state of MET protein. The transfection of ASPL-TFE3 expression plasmid into 293 cells led to an increase in both MET precursor protein (170 kDa) and its mature form (145 kDa; Fig. 2*A, arrowheads*). To exclude a nonspecific effect of transient transfection on MET protein levels, we used 293 cells stably transfected with an inducible ASPL-TFE3 construct to confirm its stimulation of MET protein expression (Fig. 2*B*). Consistent with these findings, FU-UR1 renal carcinoma cells that express the endogenous *ASPL-TFE3* fusion exhibit remarkably high expression of endogenous MET protein compared with several other types of cancer cell lines, including HeLa cervix adenocarcinoma, MCF7 breast cancer cells, A673 Ewing sarcoma cells, and three independent synovial sarcoma cell lines (SYO1, HS-SY-II, Fuji; see below; data not shown). Finally, we used phosphorylation site–specific antibody to show

that ASPL-TFE3–dependent induction of MET protein was associated with MET autophosphorylation at tyrosine residues 1,234 and 1,235 in its catalytic domain (Fig. 2*A* and *B*). In contrast, in this experiment, native TFE3 did not exhibit any effect on MET protein expression and phosphorylation (Fig. 2*A*).

ASPL-TFE3 expression triggers assembly of MET/Gab1/Crk complexes, activating downstream signaling. MET autophosphorylation at tyrosine residues 1,234 and 1,235 in the catalytic domain is followed by additional phosphorylation events at Y1349 and Y1356 in its COOH-terminal multiple-docking site, an essential step in the recruitment of downstream Gab1 (growth factor receptor binding protein 2–associated binder 1) docking protein (27). Once Gab1 is phosphorylated at multiple sites by activated MET, it can recruit several downstream transducers such as the p85 subunit of phosphatidylinositol 3-kinase (PI3K), CrkII/CrkL, PLC-γ?, Shc, SHP-2, and SHIP, leading to a variety of biological responses. Therefore, as ASPL-TFE3 expression induces MET overexpression and autophosphorylation, we next examined signaling downstream of MET in this context to better understand the biological phenotypes of ASPL-TFE3–associated tumors. MET phosphorylation at tyrosine 1,349 in its cytoplasmic multiple-docking site is known to provide a direct binding site for the Gab1 docking protein. Indeed, we were able to show that ASPL-TFE3 expression resulted in association of MET to Gab1 by immunoprecipitation analysis (Fig. 3*A*). In addition, phosphorylation at tyrosine 307 of Gab1 was induced after ASPL-TFE3 expression (Fig. 3*B*). Tyrosine 307 of Gab1 is one of the multiple binding sites for various SH2 proteins, and, indeed, this was associated with the recruitment of the adaptor protein Crk (Fig. 3*B*).

Examining more downstream phosphorylation targets in these signaling pathways, we found that ASPL-TFE3 induced the phosphorylation of p44/42 MAPK (T202/Y204) and myc (T58/S62) in 293 cells, although their total expression levels remained constant (not shown for myc; Fig. 3*C*). Phosphorylation at these sites increased at 48 h after ASPL-TFE3 induction compared with 24 h. As expected, the dominant negative form of Ras (Ras N19) blocked ASPL-TFE3–induced phosphorylation of p44/42 MAPK (Fig. 3*D*, *lanes 6* and *9*). To examine the cell specificity of this ASPL-TFE3–mediated activation of MAPK, three other cell lines, HeLa, Cos7, and MCF7, were transfected with the expression plasmids for

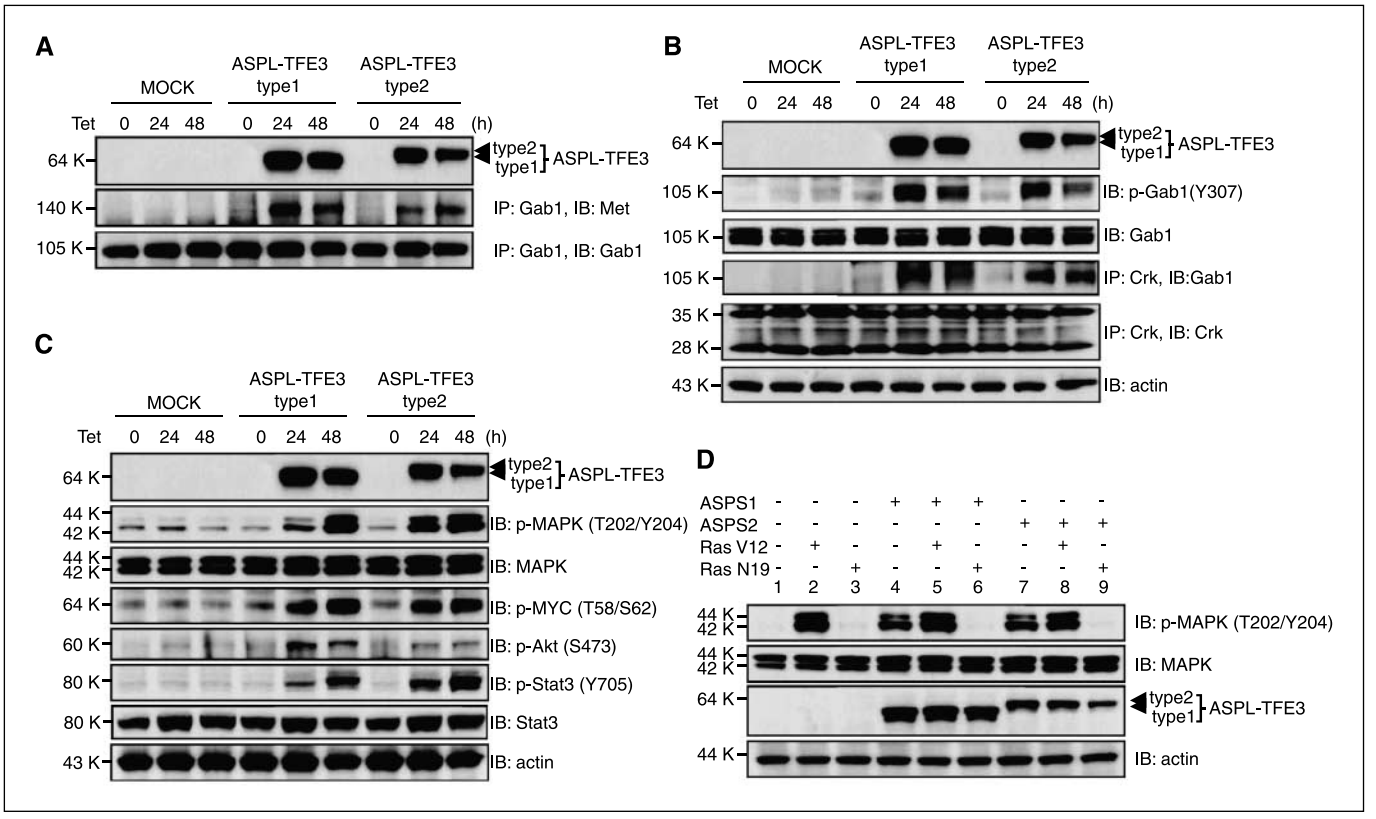

Figure 3. ASPL-TFE3 recruits MET/Gab1/Crk complexes, activating the ERK and PI3K/Stat pathways. *A,* ASPL-TFE3–induced recruitment of Gab1 to phosphorylated MET. MOCK-, ASPL-TFE3 type 1–, or ASPL-TFE3 type 2–inducible 293 cells were treated with 1 μg/mL tetracycline for 24 or 48 h, and the expression levels of ASPL-TFE3 were examined by immunoblot using anti-myc antibody. The phosphorylation at residue Y1349 of MET was analyzed by immunoprecipitation using anti-MET antibody followed by immunoblotting with phosphorylated Y1349–specific MET antibody. To detect the association of MET and Gab1, the cell lysate was immunoprecipitated with anti-Gab1 antibody, and subsequently MET bound to Gab1 was detected with anti-MET antibody. *B,* ASPL-TFE3–mediated Gab1/Crk complexes. Tetracycline treatment of ASPL-TFE3–inducible 293 cells was done as described in (*A*). The phosphorylation at the Y307 residue of Gab1 in whole-cell lysates was analyzed by immunoblotting. The association of Crk and Gab1 was examined by immunoprecipitation using anti-Crk antibody followed by immunoblotting with anti-Gab1 antibody. *C,* MOCK or ASPL-TFE3–inducible 293 cells were treated with 1 μg/mL tetracycline for 24 or 48 h, and the expression levels of ASPL-TFE3 were examined by immunoblot with anti-myc antibody. The phosphorylations of p42/44 MAPK (T202/Y204), myc (T58/S62), Akt (S473), and Stat3 (Y705) in whole-cell lysates were examined by immunoblotting with phosphorylation site–specific antibodies. The protein levels loaded in each well were confirmed with anti-MAPK, anti-Stat3, and antiactin antibodies. *D,* Ras-dependent MAPK phosphorylation in ASPL-TFE3–induced 293 cells. 293T cells were transiently transfected with the expression plasmids for ASPL-TFE3 type 1 or type 2 with or without the expression plasmids for dominant active form of Ras (Ras V12) or its dominant negative form (Ras N19), as indicated. The expression levels of ASPL-TFE3 were examined by immunoblotting with anti-myc antibody. The phosphorylations at T202/Y204 of MAPK were identified using specific antibodies.

native TFE3, ASPL-TFE3 type 1, or ASPL-TFE3 type 2. ASPL-TFE3 induced phosphorylation of MAPK in HeLa and 293 cells, but no change in MAPK phosphorylation could be detected in Cos7 and MCF7 cells, possibly due the high basal phosphorylation levels in these two cell lines (not shown).

Regarding the PI3K/Akt signaling pathway, we found that Akt and Stat3 were also phosphorylated at serine 473 and tyrosine 705, respectively, upon ASPL-TFE3 induction in 293 cells (Fig. 3*C*). In contrast, the phosphorylation of p90 RSK, Elk, MAPKAPK-2, and HSP27, all mainly related to the p38 MAPK pathway, were unresponsive to the expression of ASPL-TFE3 in its inducible 293 cells (data not shown).

Activation of MET signaling pathways in tumors with TFE3 fusions. To support the relevance of these data to human tumors *in vivo*, we confirmed that MET is detectable by both immunohistochemistry (Fig. 4*A*) and immunoblotting (Fig. 4*B*) in most ASPL-TFE3–positive clinical tumor samples. In addition, the expression levels of HGF in these tumors were also remarkably high (Fig. 4*A* and *B*). In contrast, we did not detect HGF expression in most other translocation-associated sarcomas by immunohistochemistry (data not shown). Thus, among the sarcomas tested, coexpression of MET and its ligand, HGF, was by far most frequent and most striking in ASPS.

Examining the *in vivo* activation status of signaling mediators downstream of MET by immunoblotting, we found that the high expression of MET in ASPS tumors and ASPL-TFE3–positive or PRCC-TFE3–positive renal carcinomas was associated with phosphorylation of Akt and p44/42 MAPK, at S473 and T202/Y204, respectively (Fig. 4*B*). MET expression level, phosphorylation, and activation of downstream mediators in these tumors containing TFE3 fusions was generally comparable with that observed in eight papillary renal cell carcinomas (a subtype characterized by activating *MET* mutations; not shown).

Consistent with the data from exogenous ASPL-TFE3 in heterologous cells and from clinical tumor samples, we observed that FU-UR1 cells display, in the presence of HGF, prominent phosphorylation of MET in the catalytic domain and multiple-docking site, the recruitment of Crk to phosphorylated Gab1, leading to strong phosphorylation of downstream transducers such as Raf-1 (S338), p44/42 MAPK (T202/Y204), Akt (S473), and Stat3 (Y705; Fig. 4*C*).

Effects of MET knockdown on MET-mediated signaling pathways in cells with endogenous ASPL-TFE3. To evaluate MET as a potential therapeutic target in ASPL-TFE3–associated tumors, we first used RNA interference to knock down MET. RNA interference using siRNA transfections resulted in almost complete depletion of MET protein in FU-UR1 cells (Fig. 4*C*), which completely abolished HGF-dependent phosphorylation of MET at Y1234/Y1235 and Y1349 and of downstream transducers such as Gab1 at Y307, p42/44 MAPK at T202/Y204, Akt at S473, and Stat3 at Y705 (Fig. 4*C*). Consistent with the loss of Gab1 phosphorylation, the HGF-dependent association of Crk to Gab1 was also abolished (Fig. 4*C*).

Effects of PHA665752 on MET-mediated signaling pathways in cells with endogenous ASPL-TFE3. As a complementary approach to validate MET as a potential therapeutic target in human cancers with *TFE3* fusions, we examined the effects of the selective MET inhibitor PHA665752 (18). As little as 0.5 μmol/L PHA665752 dramatically suppressed HGF-dependent MET phosphorylation at Y1234/Y1235 in FU-UR1 cells, and 1 μmol/L of this compound abolished it completely (Fig. 4*D*). Furthermore, PHA665752 was also effective in inhibiting HGF-triggered phosphorylation of downstream Gab1, Akt, and MAPK in a dose-dependent manner, and, indeed, 1 μmol/L PHA665752 suppressed phosphorylation at these sites quite potently (Fig. 4*D*). As expected, 50 μmol/L LY294002 completely inhibited HGF-dependent phosphorylation of Akt and Stat3, but did not affect Gab1 and MAPK (Supplementary Fig. S1). However, contrary to our expectations, PD98059 did not fully suppress HGF-dependent phosphorylation of MAPK in FU-UR1 cells (Supplementary Fig. S1).

MET inhibition by PHA665752 decreases cell viability and proliferation of cells with endogenous ASPL-TFE3. To evaluate the relationship between the expression levels of MET and the effects of PHA665752 on cell viability, we used five different cell lines expressing a variety of levels of endogenous MET protein. Consistent with our microarray data on clinical samples with the same fusion oncoproteins, FU-UR1 renal carcinoma cells (ASPL-TFE3–positive) and RH30 alveolar rhabdomyosarcoma cells (PAX3-FKHR–positive) exhibited remarkably higher levels of MET than A673 Ewing sarcoma cells (EWS-FLI1–positive) or the synovial sarcoma cell lines, HS-SY-II (SYT-SSX1–positive) and Fuji (SYT-SSX2–positive; Fig. 5*A*). The up-regulation of MET in alveolar rhabdomyosarcomas has been previously reported (28).

PHA665752 decreased the viability of FU-UR1 cells in a dose-dependent manner (Fig. 5*B*). The IC_{50} of PHA665752 in this cell line was 0.5 μmol/L, the lowest of the five cell lines tested. PD98059, LY294002, and rapamycin also reduced the viability of FU-UR1 cells; however, in contrast to the findings with PHA665752, for none of these other compounds was FU-UR1 the most sensitive cell line among these five lines (Supplementary Fig. S2*A*). Finally, combining the two most active compounds, PHA665752 and rapamycin, produced an additive effect on FU-UR1 cells, reducing cell counts by ~75% at 8 days (Supplementary Fig. S2*B*). A cooperative effect of PHA665752 and rapamycin has been reported in other cancers (29).

MET knockdown decreases viability and proliferation of cells with other *TFE3* fusions. To examine whether MET is also playing a similar role in cells containing other *TFE3* fusions, we depleted MET in the UOK109 and UOK145 renal carcinoma cell lines using a shRNA (Fig. 5*C*) that was delivered by either transfection or retroviral infection. Whereas control cells (HeLa) were unaffected by MET shRNA (not shown), MET knockdown potently decreased UOK109 and UOK145 cell viability (Fig. 5*D*).

MET depletion inhibits HGF-mediated phenotypes in cells with endogenous ASPL-TFE3. HGF/MET signaling is known to play important roles in cell adhesion, motility, and invasion, processes that may be determinants of metastatic potential and poor prognosis (reviewed in refs. 30, 31). HGF stimulation of FU-UR1 cells dramatically increased cell adhesion on extracellular matrix proteins such as collagen IV, fibronectin, and laminin/fibronectin (Supplementary Fig. S3*A*). The depletion of MET by RNA interference completely abrogated the HGF-triggered enhancement of cell adhesion (Supplementary Fig. S3*A*). Wound-healing assays (32) were done to evaluate the scattering and motility of FU-UR1 cells. In the absence of HGF, the cell motility after wound formation was almost equal between MOCK-, control siRNA–, and MET siRNA–transfected cells, although a slight decrease was observed in MET siRNA–transfected cells after 16 h (Supplementary Fig. S3*B*). HGF stimulation led to remarkable cell scattering and induced more than twice higher cell motility compared with that without HGF in MOCK- or control siRNA–transfected cells (Supplementary Fig. S3*B*). However, MET-depleted cells failed to dissociate from

each other even upon HGF stimulation, resulting in no significant cell movement (Supplementary Fig. S3*B*). Finally, we found that the elimination of MET by RNA interference dramatically inhibited HGF-evoked Matrigel invasion (Supplementary Fig. S3*C*), consistent with the abolishment of HGF-mediated cell adhesion to extracellular matrix, scattering, and cell motility shown above. The treatment of FU-UR1 cells with 1 μmol/L PHA665752 also completely abolished HGF-stimulated Matrigel invasion (data not shown).

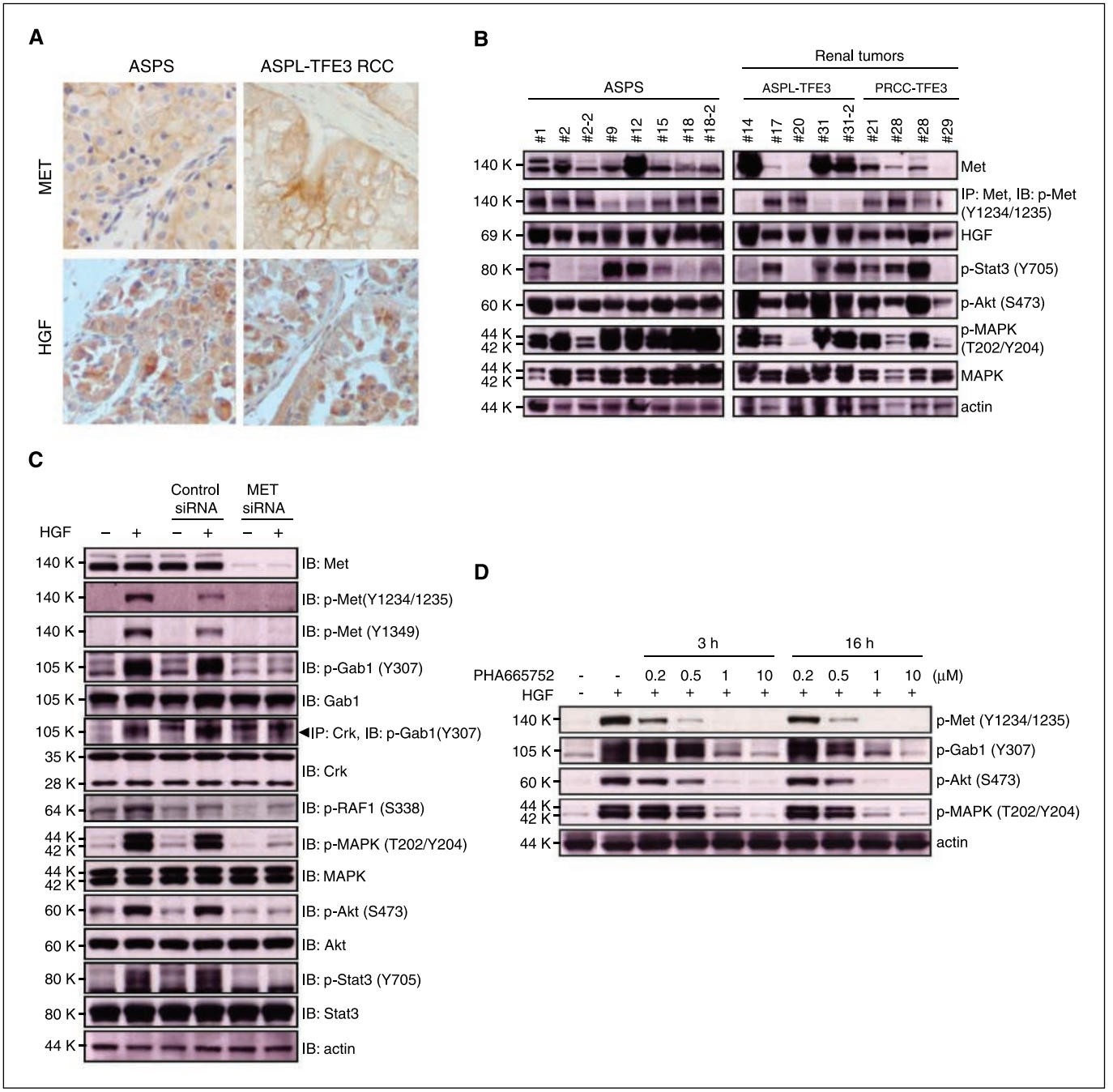

Figure 4. MET expression and activation of downstream signaling in tumors with TFE3 fusions and its inhibition by RNA interference and PHA665752. *A,* immunohistochemistry for MET showing prominent membranous and cytoplasmic expression in ASPS (*top left*) and ASPL-TFE3–positive renal carcinoma (*top right*). Note that in both images, nonneoplastic elements are negative. The immunohistochemical analysis of HGF likewise showed strong cytoplasmic positivity in ASPS cases (*bottom left*) and ASPL-TFE3–positive renal carcinomas (*top right*). *B,* the protein expression levels of MET and HGF, and the phosphorylation status of Akt, Stat3, and p44/42 MAPK were analyzed in whole-cell lysates obtained from ASPS tumors (all containing ASPL-TFE3) and ASPL-TFE3–positive renal carcinomas by immunoblotting. *C,* effects of MET depletion on HGF-dependent MET signaling cascade in FU-UR1 cells. FU-UR1 cells were transfected with MET siRNA or nonspecific siRNA as negative control. After 72 h, the cells were treated with or without 50 ng/mL HGF for 30 min, and subsequently the phosphorylation status of signaling proteins downstream of MET was analyzed by the immunoblotting with the indicated antibodies. The association of Crk and Gab1 was examined by immunoprecipitation (*IP*) using anti-Crk antibody followed by immunoblotting with anti–phosphorylated Gab1 antibody. *D,* FU-UR1 cells were treated with the MET selective inhibitor PHA665752 at the doses indicated for 3 or 16 h followed by 50 ng/mL HGF for 30 min. The phosphorylation status of MET (Y1234/1235), Gab1 (Y307), Akt (S473), and p42/44 MAPK (T202/Y204) was examined by specific antibodies.

Discussion

Aberrant activation of HGF/MET signaling has been implicated in key oncogenic phenotypes such as uncontrolled cell proliferation, invasion, and metastasis (reviewed in ref. 31). Clinically, MET overexpression or activation correlates with poor prognosis in a variety of human cancers (30), including usual (nontranslocation) renal carcinomas (33). Both HGF and MET have been reported to be constitutively overexpressed in many tumors, resulting in autocrine or paracrine activation (30). MET can also be activated in a ligand-independent manner through MET overexpression or mutation. Missense point mutations in the kinase domain of MET that lead to its constitutive activation are well described in sporadic and hereditary papillary renal carcinomas (34). Here, we have shown that MET activation may play a major role in the biology of human tumors containing TFE3 fusions, because of its aberrant transactivation by these fusion oncogenes, as summarized in Fig. 6.

The transcriptional targets of the fusion oncoproteins that function as aberrant transcription factors are likely to be central to the biology of translocation-associated human cancers. A screen for differentially expressed genes defined by expression profiling of a large set of human sarcomas allowed us to identify the *MET* gene as significantly overexpressed in ASPS relative to its level in other translocation sarcomas. We therefore examined *MET* as a direct target of transactivation by ASPL-TFE3. We provide multiple lines of evidence to support this hypothesis. Exogenous ASPL-TFE3 fusion protein binds directly to the *MET* promoter in 293 cells, strongly transactivating it. ASPL-TFE3 is also physically present at the *MET* promoter in ASPL-TFE3–transfected 293 cells. Likewise, ChIP analysis in two renal carcinoma cell lines with other *TFE3* translocations provided evidence for occupancy of the *MET* promoter by NONO-TFE3 and PSF-TFE3.

Our finding that the up-regulation of MET protein by ASPL-TFE3 in 293 cells leads to MET autophosphorylation raised the possibility that MET may be constitutively activated in human tumors with endogenous *TFE3* fusions. Indeed, in most ASPS tumors and in *ASPL-TFE3*–positive or *PRCC-TFE3*–positive renal carcinomas, we found that MET was phosphorylated at tyrosine 1,234 and 1,235 in the catalytic domain and that HGF was coexpressed. Consistent with these findings in primary tumor material, we observed that FU-UR1 cells (with endogenous ASPL-TFE3) showed strong activation of signaling pathways downstream of MET upon HGF

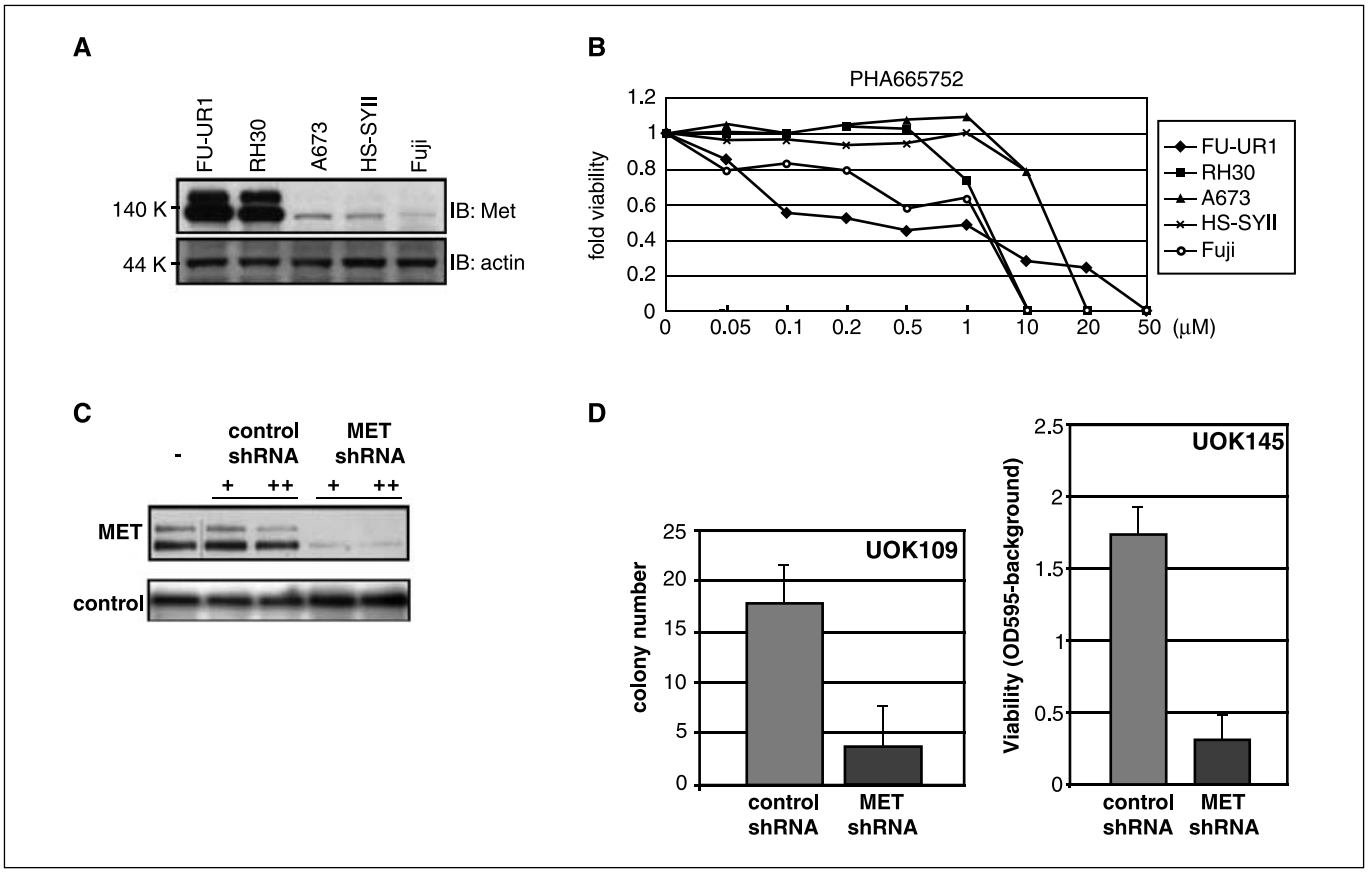

Figure 5. Effect of MET inhibition on ASPL-TFE3–mediated cell growth. *A,* the expression levels of endogenous MET protein were examined by immunoblotting in five different cell lines, including FU-UR1 renal carcinoma cells (ASPL-TFE3–positive), RH30 alveolar rhabdomyosarcoma cells (PAX3-FKHR–positive), A673 Ewing sarcoma cells (EWS-FLI1–positive), or the synovial sarcoma cell lines HS-SY-II (SYT-SSX1–positive) and Fuji (SYT-SSX2–positive). *B,* effects of MET-selective inhibitor on cell viability. Cell lines were treated with the MET-selective inhibitor PHA665752 at the indicated doses for 4 d. Live cells were counted under the microscope, and the numbers were normalized to that without inhibitor (indicated as 0 μmol/L) and described as a proportion. *C,* effects of MET depletion on growth of cells with other TFE3 fusion proteins. First, to confirm the effectiveness of the MET shRNA, COS7 cells were transfected with Flag epitope–tagged MET and LacZ together with 1 (+) or 2 (++) μg/well of pSuper expressing control or MET-directed shRNA. Whole-cell extracts were immunoblotted with anti-Flag (*MET*) or anti-LacZ (*control*). *D,* UOK109 renal carcinoma cells (NONO-TFE3 fusion positive) were transfected with pSuper directing the expression of luciferase-directed (*control*) or MET-directed shRNA together with constant amounts of pBABE-Puro. Colonies developing after puromycin selection were counted. Likewise, UOK145 renal carcinoma cells (PSF-TFE3 fusion positive), infected with retrovirus encoding luciferase-directed (*control*) or MET-directed shRNA were selected, fixed, and stained with crystal violet. Stain was eluted and quantitated (*OD595-background*). For comparison, upon the same treatment, HeLa cells were unaffected (not shown). *Bars,* SD.

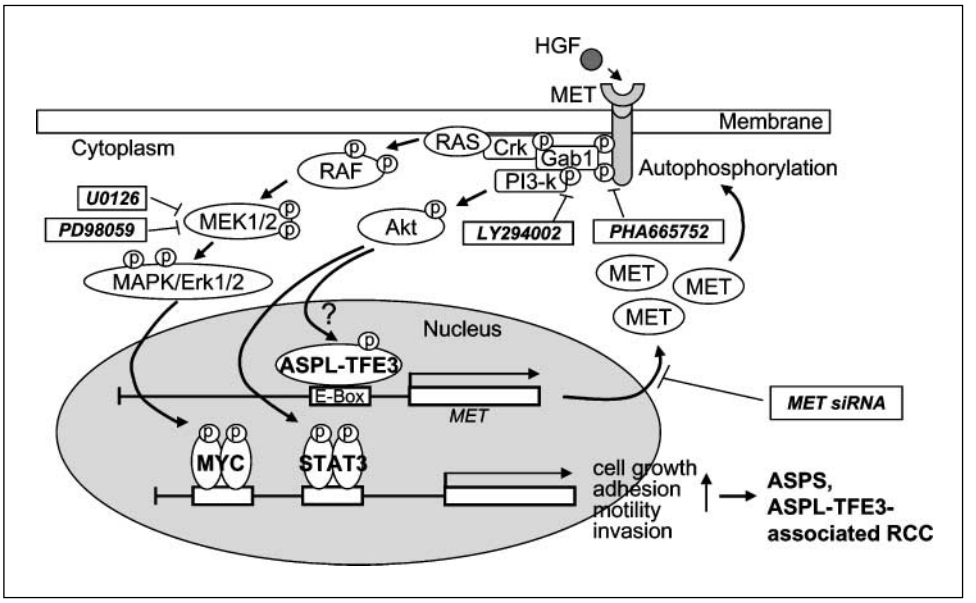

Figure 6. Proposed Schema of ASPL-TF3–mediated MET activation and downstream effects in ASPL-TFE3–containing human cancers. Various lines of Data obtained in tumors or cell lines with other *TFE3* fusions suggest that this model may be generalizable to all tumors with TFE3 fusion proteins. The possibility of positive feedback effects by phosphorylation of ASPL-TFE3 itself is shown but requires further investigation (see Discussion).

stimulation. However, we did not detect any mutations in the juxtamembrane and catalytic domains of *MET* in eight ASPS tumors and three *ASPL-TFE3*–positive renal carcinomas (data not shown).

We found that the prominent activation of MET triggered by ASPL-TFE3 expression also evoked the recruitment of phosphorylated Gab1, leading to the strong activation of downstream PI3K/Akt and Crk/Sos/Ras/extracellular signal-regulated kinase (ERK) signaling pathways (Fig. 6). PI3K/Akt signaling is a crucial pathway downstream of MET. Furthermore, PI3K bound to phosphorylated Gab1 has been reported to regulate Rac1 activity through several guanine-nucleotide exchange factors for Rac1 that are required for HGF-dependent cell motility (35). Stat3 is required for HGF/MET–mediated growth in soft agar and tumorigenesis (36), and a recent study has shown that the aberrant activation of Stat3 also contributes to MET-mediated cell motility in some cancers (37). In addition, the activation of ERKs through the Sos-Ras cascade is linked with uncontrolled proliferation, and sustained activation of this pathway is required but not sufficient for HGF-dependent motility and morphogenesis (38–40). Thus, the ASPL-TFE3 fusion oncoprotein, by transcriptionally up-regulating *MET*, may evoke various oncogenic phenotypes through the activation of the ERK and PI3K/Akt pathways.

Targeting MET in preclinical settings has been attempted using HGF-neutralizing antibodies, MET antisense oligonucleotides, dominant-negative forms of MET protein, ribozymes targeting MET mRNA, and RNA interference (29, 41). More recently, the small-molecule inhibitor PHA665752 that is selective for MET has become available (17, 29). The IC_{50} of PHA665752 against other tyrosine and serine-threonine kinases has been shown to be at least 300-fold higher than against MET, supporting it as a selective inhibitor of MET-dependent signaling pathways. In mouse tumor models, PHA665752 inhibits MET phosphorylation and downstream signal transduction and these effects correlate with tumor growth inhibition or tumor regression (18).

We achieved almost complete depletion of MET protein by RNA interference in FU-UR1 cells and this significantly reduced the effect of HGF on the PI3K/Akt and ERK pathways (Fig. 6). Furthermore, the knockdown of MET completely inhibited HGF-dependent prometastatic properties, including cell adhesion to extracellular matrix, scattering, cell motility, and Matrigel invasion, suggesting that targeting MET could affect metastatic potential, a common clinical problem in ASPS. We also examined MET inhibition by PHA665752. We found that 1 μmol/L PHA665752 strongly blocked HGF-dependent MET phosphorylation both in the catalytic domain and multifunctional docking site in FU-UR1 cells. The block in MET phosphorylation upon PHA665752 treatment suggests that this compound should also inhibit MET downstream signaling pathways and associated phenotypes. Indeed, we found that 1 μmol/L PHA665752 caused complete suppression of downstream signaling and also exhibited inhibitory effects on cell viability, proliferation, and Matrigel invasion in FU-UR1 cells. In contrast, we did not observe an equivalent effect of PHA665752 on the viability of RH30 alveolar rhabdomyosarcoma cells, in spite of their high expression of MET protein, indicating that the inhibitory effects of this compound may depend on the genetic context and cell type, which may represent an important consideration in MET-targeted therapies. Thus, based on our data, MET seems to represent a better therapeutic target in ASPS (and other tumors with TFE3 fusions) than in alveolar rhabdomyosarcomas, where MET is also up-regulated by the fusion oncoprotein (28) and has been studied as a therapeutic target (42). Overall, our data support MET as a potential therapeutic target in tumors with TFE3 fusions and provide a rationale for clinical trials of MET-targeted therapy in this tumor group.

We should note some striking parallels between the oncogenic mechanisms associated with TFE3 deregulation in the context of the ASPL-TFE3 fusion protein (and highly related fusions such as PRCC-TFE3) and MITF deregulation in cutaneous melanoma by overexpression and/or amplification. MITF is phosphorylated at serine residues in its basic-helix-loop-helix-leucine zipper (bHLH-LZ) domain and this seems to enhance its ability to activate transcription (43, 44). As the bHLH-LZ domain is highly conserved between MITF and TFE3, we explored the phosphorylation state of ASPL-TFE3. Indeed, we found that the exogenous ASPL-TFE3 is serine phosphorylated in 293T cells and FU-UR1 cells (Supplementary Fig. S4). Thus, ASPL-TFE3–evoked constitutive activation of MET signaling pathways could lead to phosphorylation of

ASPL-TFE3 by one or more pathways, thereby increasing its activity as a transcriptional activator of *MET* and other target genes, raising the possibility of a positive feedback loop. This possibility is under further investigation. Finally, this model is also supported by a recent study reporting direct transactivation of *MET* by MITF in melanocytes through binding of a site in the *MET* promoter located within the region examined in our ChIP experiments and enhancement of MITF activity by HGF/MET signaling (45), suggesting that the *MITF* amplification seen in some melanomas (46) may likewise set up a positive feedback loop that could be significant as a therapeutic target. More recently, Smolen et al. (47) have reported that gastric cancers with *MET* gene amplification (associated with ligand-independent constitutive activation) are very sensitive to PHA665752. Thus, forced overexpression of *MET* through either gene amplification (47) or aberrant transcriptional up-regulation by amplified MITF (45, 46) or by TFE3 fusion proteins, as described here, may set up a dependence on MET signaling, making tumor cells especially susceptible to MET-selective agents. Interestingly, a recent functional genetic screen led to the observation that TFE3 can counter the antiproliferative effects of transforming growth factor-β signaling in human cells (48); if TFE3 fusion proteins share this function, it could synergize with the proliferative effects of *MET* transcriptional up-regulation reported here.

More generally, specific chromosomal translocations encoding chimeric transcription factors are considered to play crucial oncogenic roles in a variety of human cancers but the fusion proteins themselves seldom represent suitable therapeutic targets. The present work shows how genes highly differentially expressed between chimeric transcription factor–associated cancers may include direct transcriptional targets of these chimeric transcription factors. Restricting such comparisons to kinase genes can help to narrow the search for direct transcriptional targets of potential therapeutic significance. The identification of kinase signaling pathways transcriptionally up-regulated by oncogenic fusion proteins may reveal more accessible therapeutic targets in this class of human cancers.

Acknowledgments

Received 8/2/2006; revised 11/7/2006; accepted 11/30/2006.

Grant support: NIH grants CA97585 (M. Ladanyi), CA102309 (D.E. Fisher), and CA100400 (I.J. Davis).

The costs of publication of this article were defrayed in part by the payment of page charges. This article must therefore be hereby marked *advertisement* in accordance with 18 U.S.C. Section 1734 solely to indicate this fact.

We thank Dr. M. Ishiguro for the FU-UR1 cell line, Dr. M. Linehan for cell lines UOK109 and UOK145, Dr. S. Tanaka for the expression plasmids of Ras V12 and Ras N19, Dr. J. Christensen for providing PHA665752, and I. Linkov and M. Asher for technical assistance with immunohistochemistry.

References

1. Ladanyi M, Lui MY, Antonescu CR, et al. The der(17)t(X;17)(p11;q25) of human alveolar soft part sarcoma fuses the TFE3 transcription factor gene to ASPL, a novel gene at 17q25. Oncogene 2001;20:48–57.

2. Argani P, Antonescu CR, Illei PB, et al. Primary renal neoplasms with the ASPL-TFE3 gene fusion of alveolar soft part sarcoma: a distinctive tumor entity previously included among renal cell carcinomas of children and adolescents. Am J Pathol 2001;159:179–92.

3. Sidhar SK, Clark J, Gill S, et al. The t(X;1)(p11.2;q21.2) translocation in papillary renal cell carcinoma fuses a novel gene PRCC to the TFE3 transcription factor gene. Hum Mol Genet 1996;5:1333–8.

4. Weterman MA, Wilbrink M, Geurts van Kessel A. Fusion of the transcription factor TFE3 gene to a novel gene, PRCC, in t(X;1)(p11;q21)-positive papillary renal cell carcinomas. Proc Natl Acad Sci U S A 1996;93: 15294–8.

5. Argani P, Antonescu CR, Couturier J, et al. PRCC-TFE3 renal tumors: morphologic, immunohistochemical, ultrastructural and molecular analysis of an entity associated with the t(X;1)(p11.2;q21). Am J Surg Pathol 2002;26:1553–66.

6. Clark J, Lu YJ, Sidhar SK, et al. Fusion of splicing factor genes PSF and NONO (p54nrb) to the TFE3 gene in papillary renal cell carcinoma. Oncogene 1997;15:2233–9.

7. Argani P, Ladanyi M. Translocation carcinomas of the kidney. Clin Lab Med 2005;25:363–78.

8. Argani P, Olgac S, Tickoo S, et al. Xp11 translocation renal cell carcinoma in adults: expanded clinical, pathologic, and genetic spectrum. Am J Surg Pathol. In press 2007.

9. Bogan JS, Hendon N, McKee AE, Tsao TS, Lodish HF. Functional cloning of TUG as a regulator of GLUT4 glucose transporter trafficking. Nature 2003;425:727–33.

10. Nagai M, Tsuda M, Saito T, Lae M, Ladanyi M. Functional properties of ASPL-TFE3 and identification of CYP17A and UPP1 as direct transcriptional targets. Proc Am Assoc Cancer Res 2005;46:1067.

11. Weterman MAJ, van Groningen JJM, Jansen A, Geurts van Kessel A. Nuclear localization and transactivating capacities of the papillary renal cell carcinoma-associated TFE3 and PRCC (fusion) proteins. Oncogene 2000; 19:69–74.

12. Skalsky YM, Ajuh PM, Parker C, et al. PRCC, the commonest TFE3 fusion partner in papillary renal carcinoma is associated with pre-mRNA splicing factors. Oncogene 2001;20:178–87.

13. Martinez-Ramirez A, Rodriguez-Perales S, Melendez B, et al. Characterization of the A673 cell line (Ewing tumor) by molecular cytogenetic techniques. Cancer Genet Cytogenet 2003;141:138–42.

14. Sonobe H, Manabe Y, Furihata M, et al. Establishment and characterization of a new human synovial sarcoma cell line, HS-SY-II. Lab Invest 1992;67:498–505.

15. Nojima T, Wang YS, Abe S, et al. Morphological and cytogenetic studies of a human synovial sarcoma xenotransplanted into nude mice. Acta Pathol Jpn 1990;40:486–93.

16. Ishiguro M, Iwasaki H, Ohjimi Y, Kaneko Y. Establishment and characterization of a renal cell carcinoma cell line (FU-UR-1) with the reciprocal ASPL-TFE3 fusion transcript. Oncol Rep 2004;11: 1169–75.

17. Du J, Miller AJ, Widlund HR, et al. MLANA/MART1 and SILV/PMEL17/GP100 are transcriptionally regulated by MITF in melanocytes and melanoma. Am J Pathol 2003;163:333–43.

18. Christensen JG, Schreck R, Burrows J, et al. A selective small molecule inhibitor of c-Met kinase inhibits c-Met-dependent phenotypes *in vitro* and exhibits cytoreductive antitumor activity *in vivo*. Cancer Res 2003;63:7345–55.

19. Mukohara T, Civiello G, Davis IJ, et al. Inhibition of the met receptor in mesothelioma. Clin Cancer Res 2005;11:8122–30.

20. Du J, Widlund HR, Horstmann MA, et al. Critical role of CDK2 for melanoma growth linked to its melanocyte-specific transcriptional regulation by MITF. Cancer Cell 2004;6:565–76.

21. Saito T, Nagai M, Tsuda M, et al. Differentially expressed genes defined by expression profiling of sarcomas with chimeric transcription factors provide an enriched source of candidate transcriptional targets. Abstracts of LXX Cold Spring Harbor Symposium 2005:225.

22. Ross ME, Zhou X, Song G, et al. Classification of pediatric acute lymphoblastic leukemia by gene expression profiling. Blood 2003;102:2951–9.

23. Robinson DR, Wu YM, Lin SF. The protein tyrosine kinase family of the human genome. Oncogene 2000;19: 5548–57.

24. Manning G, Whyte DB, Martinez R, Hunter T, Sudarsanam S. The protein kinase complement of the human genome. Science 2002;298:1912–34.

25. Clark J, Rocques PJ, Crew AJ, et al. Identification of novel genes, SYT and SSX, involved in t(X; 18)(p11.2;q11.2) translocation found in human synovial sarcoma. Nat Genet 1994;7:502–8.

26. Davis IJ, Hsi BL, Arroyo JD, et al. Cloning of an α-TFEB fusion in renal tumors harboring the t(6;11)(p21;q13) chromosome translocation. Proc Natl Acad Sci U S A 2003;100:6051–6.

27. Weidner KM, Di CS, Sachs M, et al. Interaction between Gab1 and the c-Met receptor tyrosine kinase is responsible for epithelial morphogenesis. Nature 1996; 384:173–6.

28. Ginsberg JP, Davis RJ, Bennicelli JL, Nauta LE, Barr FG. Up-regulation of MET but not neural cell adhesion molecule expression by the PAX3-FKHR fusion protein in alveolar rhabdomyosarcoma. Cancer Res 1998;58: 3542–6.

29. Ma PC, Schaefer E, Christensen JG, Salgia R. A selective small molecule c-MET Inhibitor, PHA665752, cooperates with rapamycin. Clin Cancer Res 2005;11:2312–9.

30. Birchmeier C, Birchmeier W, Gherardi E, Vande Woude GF. Met, metastasis, motility and more. Nat Rev Mol Cell Biol 2003;4:915–25.

31. Gao CF, Vande Woude GF. HGF/SF-Met signaling in tumor progression. Cell Res 2005;15:49–51.

32. Rodriguez LG, Wu X, Guan JL. Wound-healing assay. Methods Mol Biol 2005;294:23–9.

33. Miyata Y, Kanetake H, Kanda S. Presence of phosphorylated hepatocyte growth factor receptor/c-Met is associated with tumor progression and survival in patients with conventional renal cell carcinoma. Clin Cancer Res 2006;12:4876–81.

34. Schmidt L, Duh FM, Chen F, et al. Germline and somatic mutations in the tyrosine kinase domain of the MET proto-oncogene in papillary renal carcinomas. Nat Genet 1997;16:68–73.

35. Furge KA, Zhang YW, Vande Woude GF. Met receptor tyrosine kinase: enhanced signaling through adapter proteins. Oncogene 2000;19:5582–9.

36. Zhang YW, Wang LM, Jove R, Vande Woude GF. Requirement of Stat3 signaling for HGF/SF-Met mediated tumorigenesis. Oncogene 2002;21:217–26.

37. Cramer A, Kleiner S, Westermann M, et al. Activation of the c-Met receptor complex in fibroblasts drives

invasive cell behavior by signaling through transcription factor STAT3. J Cell Biochem 2005;95:805–16.
38. Khwaja A, Lehmann K, Marte BM, Downward J. Phosphoinositide 3-kinase induces scattering and tubulogenesis in epithelial cells through a novel pathway. J Biol Chem 1998;273:18793–801.
39. Tanimura S, Nomura K, Ozaki K, et al. Prolonged nuclear retention of activated extracellular signal-regulated kinase 1/2 is required for hepatocyte growth factor-induced cell motility. J Biol Chem 2002;277:28256–64.
40. Karihaloo A, O'Rourke DA, Nickel C, Spokes K, Cantley LG. Differential MAPK pathways utilized for HGF- and EGF-dependent renal epithelial morphogenesis. J Biol Chem 2001;276:9166–73.
41. Maulik G, Shrikhande A, Kijima T, et al. Role of the hepatocyte growth factor receptor, c-Met, in oncogenesis and potential for therapeutic inhibition. Cytokine Growth Factor Rev 2002;13:41–59.
42. Taulli R, Scuoppo C, Bersani F, et al. Validation of met as a therapeutic target in alveolar and embryonal rhabdomyosarcoma. Cancer Res 2006;66:4742–9.
43. Hemesath TJ, Price ER, Takemoto C, Badalian T, Fisher DE. MAP kinase links the transcription factor microphthalmia to c-Kit signalling in melanocytes. Nature 1998;391:298–301.
44. Goding C, Meyskens FL, Jr. Microphthalmic-associated transcription factor integrates melanocyte biology and melanoma progression. Clin Cancer Res 2006;12:1069–73.
45. McGill GG, Haq R, Nishimura EK, Fisher DE. c-Met expression is regulated by Mitf in the melanocyte lineage. J Biol Chem 2006;281:10365–73.
46. Garraway LA, Widlund HR, Rubin MA, et al. Integrative genomic analyses identify MITF as a lineage survival oncogene amplified in malignant melanoma. Nature 2005;436:117–22.
47. Smolen GA, Sordella R, Muir B, et al. Amplification of MET may identify a subset of cancers with extreme sensitivity to the selective tyrosine kinase inhibitor PHA-665752. Proc Natl Acad Sci U S A 2006;103:2316–21.
48. Nijman SM, Hijmans EM, El MS, et al. A functional genetic screen identifies TFE3 as a gene that confers resistance to the anti-proliferative effects of the retinoblastoma protein and transforming growth factor-β. J Biol Chem 2006;281:21582–7.